JOURNAL OF MOLECULAR SPECTROSCOPY **147,** 40–45 (1991)

The $\tilde{B}^2\Sigma^+$–$\tilde{X}^2\Sigma^+$ Transition of CaOD

R. A. HAILEY, C. N. JARMAN, W. T. M. L. FERNANDO, AND P. F. BERNATH[1]

Department of Chemistry, University of Arizona, Tucson, Arizona 85721

The $\tilde{B}^2\Sigma^+$–$\tilde{X}^2\Sigma^+$ transition of CaOD near 5550 Å was studied using dye laser excitation spectroscopy. The 000–000 band was rotationally analyzed and r_0 structures were established for both states. For the $\tilde{B}^2\Sigma^+$ state the following bond lengths were found: r_{Ca-O} = 1.9697 Å and r_{O-H} = 0.9179 Å, while for the $\tilde{X}^2\Sigma^+$ state r_{Ca-O} = 1.9849 Å and r_{O-H} = 0.9207 Å.

INTRODUCTION

The spectra of CaOH are well known because when calcium salts are added to flames, the reddish and greenish emission of CaOH is observed (*1, 2*). The red emission near 6220–6270 Å belongs to the $\tilde{A}^2\Pi$–$\tilde{X}^2\Sigma^+$ system, while the green emission near 5550 Å corresponds to the $\tilde{B}^2\Sigma^+$–$\tilde{X}^2\Sigma^+$ transition (*2*). Hilborn *et al.* (*3*) rotationally analyzed the 000–000 band of the $\tilde{A}^2\Pi$–$\tilde{X}^2\Sigma^+$ transition for both CaOH and CaOD. Bernath and Kinsey-Nielsen (*4*) analyzed the $\tilde{B}^2\Sigma^+$–$\tilde{X}^2\Sigma^+$ transition of CaOH, while Bernath and Brazier (*5*) measured some additional $\tilde{A}^2\Pi$–$\tilde{X}^2\Sigma^+$ lines and fitted the $\tilde{A}$–$\tilde{X}$ and $\tilde{B}$–$\tilde{X}$ data together.

The initial goal of our work was to investigate the highly excited electronic states of CaOH using the technique of optical–optical double resonance. Many new vibronic states were found during the course of our research, but it was necessary to differentiate the origin bands from vibrationally excited bands by using isotopic substitution. While the rotational analysis for the 000–000 band of the $\tilde{B}^2\Sigma^+$–$\tilde{X}^2\Sigma^+$ transition of CaOH is complete (*4*), the corresponding CaOD transition had not been analyzed. Consequently it was necessary to record the high-resolution spectrum of the green system of CaOD to aid in our optical–optical double resonance assignments. This paper contains the rotational analysis of the 000–000 band of $\tilde{B}^2\Sigma^+$–$\tilde{X}^2\Sigma^+$ transition of CaOD, as well as r_0 structures for both states.

EXPERIMENTAL DETAILS

The CaOD was produced in a Broida-type oven (*6*) by the reaction of Ca metal vapor and D_2O_2. It was found that the D_2O_2 produced more CaOD than D_2O in the reaction with ground state ($^1S_0$) Ca vapor. The calcium was vaporized in a resistively heated alumina crucible and a flow of argon carried the Ca atoms from the crucible to the reaction region. In order to get sufficient D_2O_2 partial pressure inside of the oven, argon was bubbled through the oxidant. The pumping speed and the flow rate

[1] Camille and Henry Dreyfus Teacher-Scholar.

0022-2852/91 $3.00

TABLE I

Measured Line Positions of the 000–000 Band of the $\tilde{B}^2\Sigma^+$–$\tilde{X}^2\Sigma^+$ Electronic Transition of CaOD (in cm^{-1})

N	P_1	O–C[a]	P_2	O–C	R_1	O–C	R_2	O–C
0					18014.491	1		
1	18013.390	2			18015.096	2	18015.192	–2
2	18012.664	–7	18012.738	5	18015.701	–5	18015.838	–9
3	18012.063	0	10812.183	17	18016.325	–3	18016.505	–4
4	18011.462	–1	18011.605	–1	18016.964	6	18017.182	2
5	18010.874	1	18011.056	–1	18017.598	1	18017.864	3
6	18010.290	–1	18010.516	0	18018.247	1	18018.547	–2
7	18009.721	2	18009.982	–2	18018.902	–1	18019.225	–21
8	18009.160	4	18009.460	–1	18019.570	0	18019.954	0
9	18008.604	2	18008.950	3	18020.246	1	18020.669	–1
10	18008.059	3	18008.444	1	18020.929	0	18021.393	–1
11	18007.515	–5	18007.947	0	18021.628	7	18022.129	2
12	18006.987	–6	18007.459	–1	18022.323	0	18022.869	0
13	18006.477	2	18006.987	5	18023.023	–10	18023.619	–1
14	18005.970	4	18006.512	–2	18023.757	4	18024.384	4
15	18005.467	1	18006.056	2	18024.477	–4	18025.149	0
16	18004.974	–1	18005.605	1	18025.216	–2	18025.921	–5
17	18004.493	0	18005.162	0	18025.974	11	18026.712	–1
18	18004.018	–2	18004.730	0	18026.712	–6	18027.506	–2
19	18003.556	0	18004.306	–1	18027.478	–3	18028.305	–7
20	18003.101	0	18003.893	1	18028.254	0	18029.134	10
21	18002.662	7	18003.491	4	18029.026	–8	18029.949	4
22	18002.219	1	18003.093	2	18029.820	–4	18030.777	2
23	18001.791	0	18002.700	–3	18030.620	–2	18031.613	–1
24	18001.371	–1	18002.322	–4	18031.434	4	18032.458	–4
25	18000.961	–2	18001.954	–2	18032.244	–1	18033.319	0
26	18000.549	–12	18001.594	–3	18033.070	1	18034.190	7
27	18000.170	0	18001.248	2	18033.899	–3	18035.054	–2
28	17999.789	1	18000.909	5	18034.742	–1	18035.937	–2
29	17999.411	–4	18000.584	13	18035.596	3	18036.831	1
30	17999.048	–2	18000.244	–3	18036.451	–1	18037.729	1
31	17998.696	1	17999.932	0	18037.317	–2	18038.635	–1
32	17998.348	–1	17999.621	–6	18038.203	8	18039.550	–3
33	17998.009	–2	17999.329	0	18039.080	0	18040.489	11
34	17997.685	2	17999.043	1	18039.974	1	18041.414	2
35	17997.363	–1	17998.764	1	18040.872	–2	18042.353	0
36	17997.055	1	17998.492	–2	18041.779	–5	18043.301	–2
37	17996.751	–1	17998.234	1	18042.699	–4	18044.269	6
38	17996.459	–2	17997.987	5	18043.628	–2	18045.229	–1
39	17996.177	0	17997.738	–1	18044.565	0	18046.210	4
40	17995.905	2	17997.503	–3	18045.511	2	18047.190	0
41	17995.644	6	17997.281	0	18046.444	–17	18048.184	1
42	17995.387	6	17997.062	–3	18047.436	15	18049.180	–4
43	17995.136	1	17996.857	–2	18048.393	3	18050.192	–1
44	17994.898	2	17996.661	0	18049.368	1		
45	17994.666	–2	17996.467	–5	18050.350	–2		
46	17994.446	–1	17996.292	0	18051.351	4		
47	17994.236	0	17996.123	1	18052.348	0		
48	17994.030	–3	17995.960	0	18053.359	1		
49	17993.835	–5	17995.809	2	18054.376	–1		
50	17993.654	–1	17995.663	0	18055.387	–16		
51	17993.478	–2	17995.526	–2				
52	17993.313	0	17995.394	–7				
53	17993.158	3	17995.290	5				
54	17993.009	3	17995.161	–16				
55	17992.867	0	17995.080	3				
56	17992.739	3	17994.988	1				
57	17992.613	–1						
58	17992.503	3						
59	17992.399	3						
60	17992.299	–1						
61	17992.210	–3						
62	17992.135	0						
63	17992.065	–1						
64	17992.004	–1						

[a] O–C corresponds to the observed minus calculated positions(in $10^3 cm^{-1}$)using the spectroscopic constants in Table II.

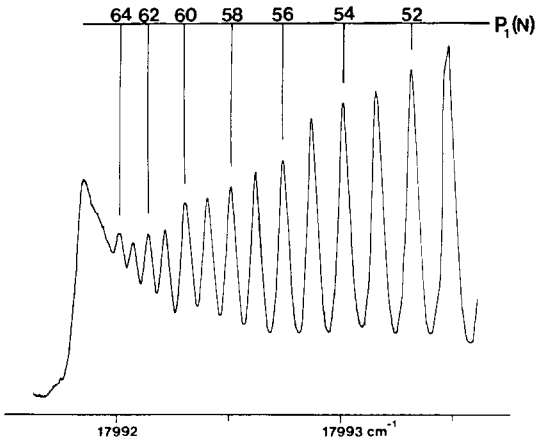

FIG. 1. High-resolution CaOD spectrum. This is a section of the laser excitation spectrum of the P_1 branch of the 000–000 band of the $\tilde{B}^2\Sigma^+$–$\tilde{X}^2\Sigma^+$ transition. The P_1 branch forms a head at 17 991.828 cm^{-1}.

were adjusted to optimize the signal. The total pressure in the oven was ~7 Torr (mostly argon and a few mTorr D_2O_2).

D_2O_2 was made by the deuteration of 30% H_2O_2. First the excess water was pumped off and then 99.9% D_2O was added to the H_2O_2. After deuteration, the mixture was concentrated by pumping off the excess water. This procedure was repeated several times.

The laser used in this experiment was a single-frequency Coherent 699-29 ring dye laser pumped by a Coherent Innova 20 argon ion laser (8W). The dye laser was operated with Rhodamine 110 dye. The laser beam was focused horizontally into the flame. Spectra were obtained by scanning the computer controlled ring dye laser while detecting the total fluorescence with a photomultiplier tube. The wavemeter of the ring dye laser was calibrated by simultaneously recording an excitation spectrum iodine vapor (*7*). The line positions have been corrected by the subtraction of 0.0056 cm^{-1} (*8*). The measured CaOD lines are listed in Table I. The estimated accuracy of the line positions is ±0.004 cm^{-1}.

RESULTS AND DISCUSSION

A portion of the laser excitation spectrum of the $\tilde{B}^2\Sigma^+$–$\tilde{X}^2\Sigma^+$ transition of CaOD near the P_1 head of the 000–000 band is shown in Fig. 1. Each $^2\Sigma^+$ state has two spin components [$F_1(e)$ and $F_2(f)$] and therefore the $^2\Sigma^+$–$^2\Sigma^+$ transition consists of four branches, P_1, P_2, R_1, and R_2 at high N (*9*). The P branches form heads at 17 991.828 and 17 994.554 cm^{-1}, for the F_1 and F_2 spin components, respectively. Because the $\tilde{X}$ and $\tilde{B}$ state potential curves are very similar the band heads occur at very high N (N = 70 for P_1 and N = 66 for P_2). The R branch region of the spectrum contains many vibrational sequence bands as well as the R_1 and R_2 branches of the 000–000 band. In order to analyze these sequence bands the technique of laser excitation spectroscopy with filtered fluorescence detection must be used.

The rotational lines of the P_1 and P_2 branches were easy to pick out, but because of the many interfering lines present in the R branch region it was difficult to pick

TABLE II

Molecular Constants for CaOD $\tilde{B}^2\Sigma^+$ and $\tilde{X}^2\Sigma^+$ States (in cm^{-1})

Parameter[a]	$\tilde{X}^2\Sigma^+$	$\tilde{B}^2\Sigma^+$
T_0	0.0	18013.894(4)
B_0	0.303004(83)	0.307488(85)
D_0	3.016(25) x 10^{-7}	3.156(26) x 10^{-7}
γ_0	0.001006[b]	-0.039536(13)

[a] One σ uncertainty in parentheses.

[b] Fixed to the value calculated from the isotopic relationship (see text).

out the *R*-branch rotational lines. The rotational assignments were made by first predicting the spectrum using an estimated band origin and molecular constants. The initial estimates were made using the previous work for CaOD (*3*) and CaOH (*5*). Then the band origin was changed until the positions of the *P* heads, as well as the pattern of the *R* rotational lines in the predicted spectrum, matched the actual line positions.

The lines were fit to the $^2\Sigma$ energy level expression using a nonlinear least-squares program. The Hund's case (a) matrix elements of the standard $^2\Sigma$ Hamiltonian (*10*) used in this analysis are listed in the paper by Douay *et al.* (*11*). Only $\gamma'-\gamma''$ is well determined, therefore for the final fit γ'' was fixed to the value obtained using the isotopic relationship

$$\gamma_{CaOD} = \gamma_{CaOH} \frac{B_{CaOD}}{B_{CaOH}}. \quad (1)$$

B_{CaOH} and γ_{CaOH} were taken from the results of Bernath and Brazier (*5*). The molecular constants from the final fit are presented in Table II.

The accuracy of Eq. (1) can be checked by substituting the γ'_{CaOD} from this work into Eq. (1), and predicting the γ'_{CaOH} value ($-0.043\,640\ cm^{-1}$). This value is identical, within experimental error, to the result from Bernath and Brazier ($-0.0436\ 15(46)$

TABLE III

Bond Lengths in CaOH and CaOD (in Å)

Bond length	$\tilde{X}^2\Sigma^+$	$\tilde{B}^2\Sigma^+$
r_0(Ca-O)	1.9849	1.9697
r_0(O-H)	0.9207	0.9179

TABLE IV

Ground State Bond Lengths for the Alkaline Earth Monohydroxides (in Å)

Bond Length	MgOH[a]	CaOH[b]	SrOH[c]	BaOH[d]
r_0(M-O)	1.770	1.984	2.111	2.201
r_0(O-H)	0.912	0.921	0.922	0.923

[a] Reference 12.

[b] This work.

[c] Reference 13.

[d] Reference 14.

cm^{-1}) (*5*). The ground state constants are in reasonable agreement with those of Hilborn *et al.* (*3*).

CaOH and CaOD are linear. Using the relationship between the moment of inertia and the bond lengths of a linear molecule

$$I = \frac{1}{M}(m_1m_2r_{12}^2 + m_1m_3r_{13}^2 + m_2m_3r_{23}^2) \tag{2}$$

the r_0 structures for CaOH in both the $\tilde{B}^2\Sigma^+$ and $\tilde{X}^2\Sigma^+$ states were determined. The moments of inertia for CaOD are calculated from the B values of Table II, while the corresponding data for CaOH were taken from the work of Bernath and Brazier (*5*). The results are presented in Table III. The bond lengths of the $\tilde{B}^2\Sigma^+$ state are shorter than in the $\tilde{X}^2\Sigma^+$ state which suggests that the nonbonding valence electron has slight antibonding character in the ground state.

For the $\tilde{X}^2\Sigma^+$ state the Ca–O bond length (1.985 Å) agrees with the value of Hilborn *et al.* (*3*), but the ground state O–H bond length (0.921 Å) is different than their value (0.901 Å). This difference reflects the slightly different B values used in our analysis, and we note that r_0 structures for hydrogen atom positions are notoriously unreliable. However, the O–H bond length obtained in this work compares quite well with the O–H bond lengths found in the other alkaline earth monohydroxides. The known bond lengths of the ground states of the alkaline earth hydroxides are provided in Table IV for comparison purposes.

ACKNOWLEDGMENT

This work was supported by the National Science Foundation (CHE-8913785).

RECEIVED: November 26, 1990

REFERENCES

1. J. F. W. HERSCHEL, *Trans. R. Soc. Edinburgh* **9**, 445–460 (1823).
2. C. G. JAMES AND T. M. SUGDEN, *Nature (London)* **175**, 333–334 (1955).
3. R. C. HILBORN, Q. ZHU, AND D. O. HARRIS, *J. Mol. Spectrosc.* **97**, 73–91 (1983).

4. P. F. BERNATH AND S. KINSEY-NIELSEN, *Chem. Phys. Lett.* **105,** 663–666 (1984).
5. P. F. BERNATH AND C. R. BRAZIER, *Astrophys. J.* **288,** 373–376 (1985).
6. J. B. WEST, R. S. BRADFORD, J. D. EVERSOLE, AND C. R. JONES, *Rev. Sci. Instrum.* **46,** 164–168 (1975).
7. S. GERSTENKORN AND P. LUC, "Atlas du spectra d'absorption de la molecule d'iode," CNRS, Paris, 1978.
8. S. GERSTENKORN AND P. LUC, *Rev. Phys. Appl.* **14,** 791–796 (1979).
9. G. HERZBERG, "Spectra of Diatomic Molecules," 2nd ed., Van Nostrand–Reinhold, New York, 1950.
10. R. N. ZARE, A. L. SCHMELTEKOPF, W. J. HARROP, AND D. L. ALBRITTON, *J. Mol. Spectrosc.* **46,** 37–66 (1973).
11. M. DOUAY, S. A. ROGERS, AND P. F. BERNATH, *Mol. Phys.* **64,** 425–436 (1988).
12. Y. NI, Ph.D. thesis, University of California, Santa Barbara, 1986; and D. O. Harris and T. C. Steimle, private communication.
13. J. NAKAGAWA, R. F. WORMSBECHER, AND D. O. HARRIS, *J. Mol. Spectrosc.* **97,** 37–64 (1983).
14. S. KINSEY-NIELSEN, C. R. BRAZIER, AND P. F. BERNATH, *J. Chem. Phys.* **84,** 698–708 (1986).